$$E^T \approx E^0 - kT\sum_l (\gamma_l)^2 \quad (7)$$

where E^0 is Young's modulus at room temperature and k is the Boltzmann constant. γ_l is the Grüneisen constant for the vibrational mode l subjected to the strain ϵ or stress σ and defined by

$$\gamma_l = -\frac{1}{\tilde{\nu}_l}\left(\frac{\partial \tilde{\nu}_l}{\partial \epsilon}\right) = -\frac{1}{\tilde{\nu}_l}\left(\frac{\partial \tilde{\nu}_l}{\partial \sigma}\right)E^T \quad (8)$$

Equation 7 expresses a decrease in modulus with increasing temperature. Using the shift factors ($\Delta\tilde{\nu}/\Delta\sigma$) observed for polyDCHD, the mode Grüneisen constant is evaluated as

$$\nu(C{\equiv}C) \qquad \gamma_l = 1.2$$
$$\nu(C{=}C) \qquad \gamma_l = 0.2$$
$$\nu(C{-}C) \qquad \gamma_l = 1.2$$
$$\delta(C{-}C{=}C) \qquad \gamma_l = 0.7$$

Thus a slope $\Delta E/\Delta T$ is obtained in a rough estimation as

$$\Delta E/\Delta T = -k\sum_l (\gamma_l)^2 \approx -9 \times 10^{-5}\ \mathrm{GPa/K}$$

where the temperature dependence of γ_l is assumed to be small.

Thus estimated $\Delta E/\Delta T$ is too small to interpret the observed temperature dependence of the modulus, suggesting that, in the variation of Young's modulus with temperature, the contribution of the bond stretching and bond angle deformation modes of the skeletal chain is negligibly small. In other words, we must search for other types of vibrational modes which govern the temperature behavior of the modulus at high weight. One possibility may be a skeletal torsional mode which could not be observed by the present Raman and IR measurements. In a previous paper,[7] we have developed a theory in which a decrease in the modulus with increasing temperature was interpreted on the basis of an idea of large-amplitude thermal fluctuation motion of the fully extended chain. The torsional modes around the skeletal bonds are considered to correlate with such a flexual chain motion. We are now trying to investigate how and to what extent this vibrational mode of τ(skeletal) affects the temperature and stress dependences of Young's modulus of the PDA chain.

Registry No. DCHD (homopolymer), 69289-06-1; DCHD (SRU), 66336-91-2.

References and Notes

(1) Clements, J.; Jakeways, R.; Ward, I. M. *Polymer* **1978**, *19*, 639.
(2) Geil, P. H. *Polym. Colloq. Kyoto* **1977**, 48. Hasegawa, H.; Hagerling, C. W.; Hoffman, R. W.; Geil, P. H. *Polym. Prepr. Jpn.* **1979**, *28*, 1870.
(3) Wegner, G. *Pure Appl. Chem.* **1977**, *49*, 443.
(4) Mitra, V. K.; Risen, W.; Baughman, R. H. *J. Chem. Phys.* **1977**, *66*, 2731.
(5) Batchelder, D. N.; Bloor, D. *J. Polym. Sci., Polym. Phys. Ed.* **1979**, *17*, 569.
(6) Galiotis, C.; Young, R. J.; Batchelder, D. N. *J. Polym. Sci., Polym. Phys. Ed.* **1983**, *21*, 2483.
(7) Ii, T.; Tashiro, K.; Kobayashi, M.; Tadokoro, H. *Macromolecules* **1987**, *20*, 552.
(8) Tashiro, K.; Kobayashi, M.; Tadokoro, H. *Macromolecules* **1977**, *10*, 731.
(9) Yee, K. C.; Chance, R. R. *J. Polym. Sci., Polym. Phys. Ed.* **1978**, *16*, 431.
(10) Kennedy, R. J.; Chalmers, I. F.; Bloor, D. *Makromol. Chem., Rapid Commun.* **1980**, *1*, 357.
(11) Apgar, P. A.; Yee, K. C. *Acta Crystallogr., Sect. B: Struct. Crystallogr. Cryst. Chem.* **1978**, *B34*, 957.
(12) Lewis, W. F.; Batchelder, D. N. *Chem. Phys. Lett.* **1979**, *60*, 232.
(13) Tadokoro, H. *Structure of Crystalline Polymers*; Wiley-Interscience: New York, 1979.
(14) Enkelmann, V. *Adv. Polym. Sci.* **1984**, *63*, 91.
(15) Tashiro, K.; Kobayashi, M.; Tadokoro, H. *Macromolecules* **1977**, *10*, 413.
(16) Enkelmann, V.; Leyrer, R. J.; Schleier, G.; Wegner, G. *J. Mater. Sci.* **1980**, *15*, 168.
(17) Galiotis, C.; Reed, R. T.; Yeung, P. H. G.; Young, R. J.; Chalmers, I. F.; Bloor, D. *J. Polym. Sci., Polym. Phys. Ed.* **1984**, *22*, 1589.
(18) Tashiro, K.; Kobayashi, M.; Tadokoro, H. *Polym. J.*, in press.

Structure Analysis of Polyisobutylene Based on the Whole-Pattern Fiber Diffraction Method. 1. Intensity Distribution Functions

Pio Iannelli and Attilio Immirzi*

Dipartimento di Fisica, Università di Salerno, I-84100 Salerno, Italy.

Received January 6, 1988; Revised Manuscript Received June 8, 1988

ABSTRACT: The structure of polyisobutylene crystallized under stretching has been used to verify the feasibility of the "whole-pattern" approach to structure refinement problems based on the X-ray fiber diffraction pattern, a novel procedure recently introduced by us. This paper is concerned specifically with the analysis of the resolved peaks of the spectrum for establishing empirically appropriate intensity distribution functions by means of parametrized functions and the dependence of the parameters themselves on the positions of the peaks on the spectrum.

Introduction

In previous papers[1,2] we have introduced a novel method for performing crystal structure refinements of fibrous materials which consists of using, instead of "integrated" diffraction intensities, the "whole diffraction pattern" (dp). This new approach can be considered an extension of Rietveld's method[3,4] from the powder case (one-dimensional dp) to the fiber case (two-dimensional dp).

At present we have considered the X-ray dp recorded by photographic techniques and digitized by a photoscan instrument. The method is potentially applicable, however, also with other recording techniques (e.g., counter techniques, X-ray television cameras, etc.) as well as to other radiation sources such as synchrotron radiation.

A basic question which arises is the choice of proper distribution functions for the diffracted intensity in *two directions*: along the increasing Bragg angle and along the constant Bragg angle directions. As discussed in a previous paper[1] a possible choice is to refer the intensity to the proper pair of curvilinear film coordinates (ρ,τ lines; τ are

0024-9297/89/2222-0196$01.50/0

the 2ϑ-constant lines, ρ the lines orthogonal to the former) which depend on the actual diffraction geometry: flat or cylindrical camera, fiber-axis to camera-axis orientation, etc.

In the cited work[1] we have shown, on empirical grounds, that in the case of isotactic polypropylene (IPP) and flat-camera recording Gauss functions are adequate for expressing the intensity distribution in both directions with two different peak widths H_ρ and H_τ. On this basis a whole-pattern structure refinement performed subsequently gave reliable results.[2] With IPP, however, only a few resolved reflections are present and the problem of finding the dependence of peak widths H_ρ and H_τ on the position of the peak on the film was not satisfactorily resolved.

The present study, for which preliminary results have been reported,[6] concerns the application of the method to the structure refinement of polyisobutylene (PIB) crystallized under stretching and has been undertaken starting from the work by Tadokoro et al.,[5] with the following goals: (i) to inquire more deeply on the still open question of intensity distribution functions in better conditions of resolution and considering also the cylindrical-camera case; (ii) to establish how the two peak widths (in two directions) for each peak vary with the position of the reflection on the film (in general, if more flexible distribution functions are considered (e.g., Pearson functions), the dependence of *all* parameters appearing in the parametrized distribution functions on the film coordinates must be clarifyied; PIB is a more promising choice because there are numerous resolved peaks well distributed on the film); (iii) to test and compare various models of constrained refinement suited for reducing the number of unknowns and taking into account the a priori structural information available.

In this paper we report the analysis according to the points (i) and (ii) of isolated regions of the spectrum corresponding to resolved Bragg reflections or to pairs of reflections close to each other. In the following article[7] the results of the structural refinement will be given.

Experimental Section

The PIB used in this study was the high-molecular-weight commercial product by EGA-Chemie (Catalog no. 18 149-8, mw $\approx$ 200 000).

The X-ray fiber diffraction pattern (Ni-filtered Cu Kα radiation) was recorded by using a cylindrical camera (radius 28.65 mm), taking four distinct spectra with exposures in the ratios 1.00, 2.67, 26.7, and 80.0. Each film (Eastman Kodak DEF-5) was digitized by a photoscan instrument (Optronics System P-1000, Model 30D) according to a 100 × 100 μm grid. The preliminary data processing for obtaining intensity data from the optical density measurements was taken according to the procedure outlined in ref 2. As in the preceding work the background intensity due to the incoherent scattering and to the amorphous material was not subtracted ab initio and was considered at the subsequent least-square-fitting stage.

Analysis of Individual Diffraction Peaks

The diffraction spectrum of PIB has been first analyzed peak-by-peak in order to establish appropriate intensity distribution functions (idf).

By use of the ρ,τ curvilinear film coordinates,[1] the image on the film of a single resolved reflection becomes inscribed in a rectangle and the two-variable idf can be assumed to be factorizable in two one-variable functions:

$$\Omega(\tau_i, \rho_i) = f_\tau(\tau_i - \tau_k) f_\rho(\rho_i - \rho_k) \quad (1)$$

being τ_i,ρ_i the coordinates of the ith point and τ_k,ρ_k the coordinates of the Bragg position. The functions f_τ and f_ρ could have either different functional forms or the same form with different parameters.

As already pointed out[1] if the choice of each one-dimensional idf is confined among Cauchy, Lorentz, and Gauss functions, it is practical to consider, in order to establish the proper idf empirically, the three-parameter function

$$f_{H,m,s} = \frac{C_{ms}}{H}[2^{-s}(2^{1/m} - 1) + |z|^s]^{-m} \quad (2)$$

where H is alternatively H_ρ (peak width along ρ) or H_τ (peak width along τ) and z is alternatively $(\rho_i - \rho_k)/H_\rho$ or $(\tau_i - \tau_k)/H_\tau$. For $s = 2$ the above function is Pearson-VII and so generalizes Cauchy ($m = 1$), Lorentz ($m = 2$), and Gauss ($m = \infty$) functions,[8] while $s > 2$ modifies its shape (with the same half-heigth peak width) toward a step function. C_{ms} is a normalization factor making $\int f_{H,m,s}\, dz = 1$.

With the same outline already used in a preceding study[1] we have performed a multiple regression procedure based on the least-squares method, considering regions of the film containing either a single isolated reflection or, alternatively, a pair of reflections close to each other. Regression was done by comparing the observed intensities $I_{obsd,i}$ with the calculated ones according to the following relationship (valid for reflections in pairs):

$$I_{calcd,i} = BI_k f_\tau f_\rho + I'_k f'_\tau f'_\rho \quad (3)$$

where B is a background intensity (see later), f_τ and f_ρ have the functional form (2) with the proper H_ρ and H_τ values, and I_k, I'_k are the integrated intensities. The latter are treated here as independent adjustable quantities; in a structure refinement process they will be treated as quantities proportional to the squared structure amplitudes.

The least-square procedure adopted minimizes $\chi^2 = \sum_i (1/\sigma_i^2)(I_{obsd,i} - I_{calcd,i})^2$ by means of the Gauss–Newton method[9] and can adjust the quantities I_k, H_τ, H_ρ, m_τ, m_ρ, s_τ, and s_ρ, as well as r_k and φ_k, which are the polar coordinates of the Bragg point on the film. The use of the r_k,φ_k pair instead of the curvilinear τ_k,ρ_k coordinates, for the Bragg point only, has been preferred for simplifying computation since the analytical relationships between τ,ρ and the Cartesian coordinates (see ref 2) are rather complicated. In two-reflection runs also I'_k,r'_k, and φ'_k are adjusted while H, m, and s values were not distinguished between paired reflections since the dependence on position is presumably weak.

Background intensity B depends on position on the film and in general is not a 2ϑ function only since stretching can induce orientation also in the amorphous material (that occurs, for instance, in isotactic polypropylene[2]). In the present case, however, background (including the amorphous halo) is clearly isotropic and B is a function of 2ϑ only. As at low ϑ angles ($\approx$7.3°) where 2ϑ-constant lines are very close to circles, B can be treated as a function of the polar coordinate r, independent of φ. Within a single reflection (or a pair) a linear dependence represents a good approximation:

$$B = B_0 + q(r - r_0) \quad (4)$$

with $r_0 = {}^1/_2(r_k + r'_k)$ (two-reflection runs) or $r_0 = r_k$ (one-reflection runs).

In a first stage the ls refinement was run by assuming $s = 2$ for both f_ρ and f_τ functions. In all cases and similarly to the case of IPP[1] the "refined" m exponent attains high values (>20), showing that Gauss profiles are adequate (the Pearson-VII function with $m = \infty$ is actually indistin-

Table I
Analysis of Intensity Distribution over Isolated Film Regions[a]

	reflection; no. of points							
	110 + 020; 171		220 + 040; 861		310 + 240 + 150; 861		330 + 060; 1281	
	$s = 2$	$s \neq 2$	$s = 2$	$s \neq 2$	$s = 2$	$s \neq 2$	$s = 2$	$s \neq 2$
B_0	99 (10)	129 (10)	28.79 (4)	28.69 (4)	28.03 (5)	28.03 (5)	23.43 (3)	23.36 (3)
q	28 (18)	20 (17)	0.44 (5)	0.47 (5)	−1.34 (5)	−1.33 (5)	−1.44 (4)	−1.50 (4)
I_k	79 (1)	75 (1)	35.5 (8)	43 (1)	117 (1)	144 (3)	73 (1)	87 (2)
r_k	7.296 (1)	7.297 (1)	14.862 (4)	14.866 (4)	19.825 (2)	19.825 (2)	22.639 (3)	22.641 (3)
φ_k	1.5797 (3)	1.5797 (3)	1.5693 (9)	1.5689 (8)	1.5712 (5)	1.5719 (4)	1.5700 (7)	1.5714 (6)
$H_\rho^\bullet$, H_ρ	0.462 (4)	0.468 (4)	0.45 (1)	0.50 (1)	0.531 (6)	0.554 (6)	0.522 (8)	0.566 (9)
$H_\tau^\bullet$, H_τ	0.953 (9)	0.963 (9)	1.59 (3)	1.21 (7)	2.54 (3)	1.86 (6)	2.81 (4)	1.94 (9)
s_ρ		2.17 (4)		2.4 (1)		2.21 (5)		2.33 (9)
s_τ		2.16 (4)		1.11 (7)		1.05 (4)		1.06 (5)
R index	0.050	0.048	0.020	0.019	0.022	0.019	0.027	0.025
χ^2	203	173	633	555	679	448	1414	1157
χ^2/N_p	1.19	1.01	0.74	0.64	0.79	0.52	1.10	0.90

	reflection; no. of points							
	201 + 131; 533		141; 861		122; 969		222 + 042; 1071	
	$s = 2$	$s \neq 2$	$s = 2$	$s \neq 2$	$s = 2$	$s \neq 2$	$s = 2$	$s \neq 2$
B_0	31.12 (9)	31.18 (9)	28.88 (4)	28.91 (4)	37.4 (1)	37.5 (1)	29.83 (4)	29.85 (4)
q	0.26 (13)	0.28 (13)	0.06 (4)	0.04 (5)	−4.08 (8)	−4.18 (8)	0.15 (5)	0.15 (5)
I_k	24 (1)	22 (1)	46 (8)	45 (1)	77 (1)	74 (1)	25 (1)	24 (1)
r_k	13.071 (8)	13.068 (8)	16.416 (3)	16.416 (3)	10.781 (3)	10.782 (3)	15.664 (7)	15.666 (7)
φ_k	1.387 (1)	1.388 (1)	1.4283 (5	1.4283 (5)	1.1238 (6)	1.1239 (6)	1.262 (1)	1.262 (1)
$H_\rho^\bullet$, H_ρ	0.49 (2)	0.55 (2)	0.480 (7)	0.48 (1)	0.555 (8)	0.58 (1)	0.44 (2)	0.48 (2)
$H_\tau^\bullet$, H_τ	1.06 (4)	1.20 (5)	1.47 (2)	1.51 (3)	1.10 (2)	1.19 (2)	1.30 (5)	1.46 (6)
s_ρ		3.1 (4)		2.07 (9)		2.19 (9)		2.6 (3)
s_τ		2.8 (3)		2.16 (8)		2.4 (1)		2.7 (3)
R index	0.025	0.024	0.019	0.019	0.039	0.038	0.029	0.029
χ^2	593	567	497	495	2040	1967	1594	1571
χ^2/N_p	1.11	1.06	0.58	0.57	2.10	2.02	1.49	1.47

	reflection; no. of points									
	113 + 023; 861		213; 861		204 + 134; 779		224 + 044; 861		234; 629	
	$s = 2$	$s \neq 2$	$s = 2$	$s \neq 2$	$s = 2$	$s \neq 2$	$s = 2$	$s \neq 2$	$s = 2$	$s \neq 2$
B_0	41.6 (4)	42.1 (4)	30.47 (9)	30.52 (9)	29.10 (7)	29.13 (8)	28.4 (1)	28.4 (1)	29.26 (7)	29.29 (7)
q	−4.5 (2)	−4.8 (2)	−0.16 (9)	−0.17 (9)	0.19 (6)	0.18 (6)	0.20 (7)	0.19 (7)	−1.42 (8)	−1.42 (8)
I_k	751 (10)	734 (10)	32 (2)	31 (2)	68 (2)	66 (2)	45 (2)	44 (3)	29 (1)	28 (1)
r_k	10.306 (2)	10.305 (2)	15.30 (1)	15.29 (1)	16.409 (5)	16.410 (5)	18.104 (8)	18.106 (8)	20.111 (8)	20.109 (7)
φ_k	0.7932 (3)	0.7932 (3)	1.078 (2)	1.078 (2)	0.9257 (8)	0.9258 (8)	1.006 (2)	1.006 (2)	1.059 (1)	1.059 (1)
$H_\rho^\bullet$, H_ρ	0.639 (5)	0.673 (7)	0.50 (3)	0.54 (3)	0.55 (1)	0.56 (2)	0.57 (2)	0.59 (3)	0.45 (2)	0.50 (2)
$H_\tau^\bullet$, H_τ	1.082 (9)	1.10 (1)	1.19 (6)	1.37 (8)	1.60 (4)	1.66 (5)	2.14 (9)	2.2 (1)	1.56 (6)	1.75 (7)
s_ρ		2.31 (5)		2.5 (3)		2.0 (1)		2.2 (2)		2.4 (4)
s_τ		2.07 (5)		2.9 (4)		2.3 (1)		2.1 (3)		2.8 (4)
R index	0.094	0.092	0.041	0.041	0.034	0.033	0.031	0.031	0.032	0.032
χ^2	1488	1423	3201	3164	1465	1456	1517	1515	1058	1031
χ^2/N_p	1.73	1.65	3.72	3.67	1.88	1.87	1.76	1.76	1.68	1.64

	reflection; no. of points									
	314 + 244 + 154; 779		015; 1131		125; 651		205 + 135; 861		225 + 045; 651	
	$s = 2$	$s \neq 2$	$s = 2$	$s \neq 2$	$s = 2$	$s \neq 2$	$s = 2$	$s \neq 2$	$s = 2$	$s \neq 2$
B_0	24.78 (7)	24.86 (6)	31.2 (1)	31.8 (1)	25.87 (8)	25.94 (9)	27.50 (4)	27.53 (5)	27.20 (4)	27.23 (4)
q	−2.85 (6)	−2.88 (6)	−1.65 (8)	−1.83 (8)	−0.56 (6)	−0.59 (6)	−0.84 (3)	−0.85 (3)	−0.55 (4)	−0.55 (3)
I_k	85 (2)	85 (2)	335 (3)	320 (3)	75 (2)	74 (2)	67 (1)	66 (2)	44 (1)	42 (1)
r_k	22.606 (4)	22.607 (4)	13.106 (2)	13.107 (2)	16.149 (5)	16.149 (5)	18.387 (4)	18.387 (4)	19.966 (5)	19.966 (5)
φ_k	1.1188 (7)	1.1188 (6)	0.2019 (4)	0.2018 (4)	0.6556 (7)	0.6555 (7)	0.8038 (7)	0.8037 (7)	0.8797 (8)	0.8797 (8)
$H_\rho^\bullet$, H_ρ	0.541 (9)	0.59 (1)	0.792 (6)	0.880 (8)	0.70 (1)	0.73 (2)	0.62 (1)	0.65 (1)	0.56 (1)	0.59 (2)
$H_\tau^\bullet$, H_τ	2.34 (4)	2.17 (6)	1.75 (1)	1.79 (2)	1.60 (3)	1.53 (5)	1.93 (3)	1.89 (4)	1.88 (4)	1.96 (5)
s_ρ		2.5 (1)		2.57 (4)		2.3 (1)		2.3 (1)		2.3 (1)
s_τ		1.66 (9)		2.18 (5)		1.8 (1)		1.9 (1)		2.3 (2)
R index	0.032	0.031	0.045	0.042	0.031	0.031	0.024	0.024	0.025	0.025
χ^2	1095	1040	3959	3419	870	856	748	741	779	770
χ^2/N_p	1.41	1.34	3.50	3.02	1.34	1.31	0.87	0.86	0.90	0.89

	reflection; no. of points[b]									
	(212) + (202 + 132); 1071		(312 + 242 + 152) + (322); 1581		(233) + (143); 2501		(115 + 025) + (105); 2501		(235) + (145); 861	
	$s = 2$	$s \neq 2$	$s = 2$	$s \neq 2$	$s = 2$	$s \neq 2$	$s = 2$	$s \neq 2$	$s = 2$	$s \neq 2$
B_0	31.3 (1)	31.4 (1)	26.97 (5)	26.94 (6)	29.52 (6)	29.57 (6)	29.37 (4)	29.47 (4)	26.04 (4)	26.02 (4)
q	−0.5 (1)	−0.6 (1)	−2.09 (4)	−2.08 (4)	−0.02 (4)	−0.03 (4)	−0.91 (2)	−0.92 (2)	−1.84 (3)	−1.84 (3)
I_k	28 (1)	27 (1)	35 (2)	37 (2)	67 (1)	66 (1)	415 (4)	402 (4)	47 (1)	50 (1)
r_k	13.77 (1)	13.77 (1)	20.530 (9)	20.526 (9)	17.467 (4)	17.987 (4)	14.177 (3)	14.172 (3)	21.106 (5)	21.104 (5)
φ_k	1.223 (2)	1.223 (2)	1.335 (2)	1.336 (2)	1.1568 (8)	1.1569 (8)	0.4402 (5)	0.4404 (5)	0.9228 (8)	0.9232 (2)
I'_k	48 (2)	45 (2)	33 (1)	34 (2)	78 (1)	75 (1)	185 (3)	187 (3)	43 (1)	46 (1)

Table I (Continued)

	reflection; no. of points[b]									
	(212) + (202 + 132); 1071		(312 + 242 + 152) + (322); 1581		(233) + (143); 2501		(115 + 025) + (105); 2501		(235) + (145); 861	
	$s = 2$	$s \neq 2$	$s = 2$	$s \neq 2$	$s = 2$	$s \neq 2$	$s = 2$	$s \neq 2$	$s = 2$	$s \neq 2$
r^r_k	14.232 (9)	14.239 (9)	21.588 (9)	21.58 (1)	18.770 (4)	18.768 (4)	14.668 (7)	14.672 (5)	21.853 (6)	21.854 (6)
φ'_k	1.227 (1)	1.227 (1)	1.337 (2)	1.338 (2)	1.1728 (7)	1.1729 (7)	0.5101 (9)	0.5080 (8)	0.9425 (8)	0.9419 (8)
$H_\rho^\bullet$, H_ρ	0.43 (2)	0.47 (1)	0.55 (2)	0.57 (2)	0.507 (7)	0.54 (1)	0.749 (7)	0.828 (9)	0.578 (8)	0.60 (1)
$H_\tau^\bullet$, H_τ	1.18 (3)	1.31 (5)	2.27 (8)	2.1 (1)	1.73 (2)	1.72 (4)	1.49 (1)	1.62 (2)	2.27 (4)	2.210 (5)
s_ρ		2.7 (3)		2.2 (2)		2.4 (1)		2.52 (5)		2.2 (1)
s_τ		2.6 (2)		1.7 (2)		2.00 (8)		2.30 (5)		1.58 (7)
R index	0.046	0.045	0.035	0.035	0.030	0.029	0.047	0.045	0.023	0.023
χ^2	4391	4296	3287	3276	2085	2060	8094	7622	3030	2954
χ^2/N_p	4.10	4.01	2.08	2.07	1.64	1.62	3.24	3.05	2.38	2.32

[a] Each region is delimited by a rectangle of film containing the given number of points (100 μm × 100 μm grid). The distribution function (2) is used with $m = 20$ (Gauss profiles). R index is defined as $\sum|I_{obsd,i} - I_{calcd,i}|/\sum I_{obsd,i}$. The r_k coordinates are in millimeters and φ_k in radians. Standard errors are given in parentheses. [b] The following five are two-peak regions.

Table II
Correlation Coefficients, Coefficients of Multiple Regression, and Regressions of Peak Widths H_ρ, H_τ (Values for $s \neq 2$), $H_\rho^\bullet$, $H_\tau^\bullet$ (Values for $s = 2$), s_ρ, and s_τ Parameters Versus Peak Positions[a]

			defn of correlation coeff r_{xy} and coeff of multiple regression $R_{z(xy)}$							
			$r_{xy} = \sum(x_i - \bar{x})(y_i - \bar{y})/(\sum(x_i - \bar{x})^2)^{1/2}(\sum(y_i - \bar{y})^2)^{1/2}$				$R_{z(xy)}^2 = (r_{zx}^2 + r_{zy}^2 - 2r_{zx}r_{xy}r_{yz})/(1 - r_{xy}^2)$			
			$r_{H_\rho^\bullet,r_k} = -0.065$	$r_{H_\tau,r_k} = 0.884$	$r_{H_\rho^\bullet,\varphi_k} = 0.848$	$r_{H_\tau,\varphi_k} = 0.168$	$R_{H_\rho^\bullet(r_k,\varphi_k)} = 0.720$	$R_{H_\tau(r_k,\varphi_k)} = 0.858$		
			$r_{H_\tau^\bullet,r_k} = 0.872$	$r_{s_\rho,r_k} = -0.256$	$r_{H_\tau^\bullet,\varphi_k} = -0.099$	$r_{s_\rho,\varphi_k} = -0.078$	$R_{H_\tau^\bullet(r_k,\varphi_k)} = 0.761$	$R_{s_\rho(r_k,\varphi_k)} = -0.068$		
			$r_{H_\rho,r_k} = -0.088$	$r_{s_\tau,r_k)} = -0.486$	$r_{H_\rho,\varphi_k} = 0.859$	$r_{s_\tau,\varphi_k} = -0.119$	$R_{H_\rho(r_k,\varphi_k)} = 0.738$	$R_{s_\tau(r_k,\varphi_k)} = 0.278$		
									S	R
regression	H'_ρ	(5 cost.)	$\mu_{\rho 0} = 0.72$ (19)	$\mu_{\rho 1} = -0.036$ (22)	$\mu_{\rho 2} = 0.0011$ (7)		$\mu_{\rho 3} = 0.057$ (104)	$\mu_{\rho 4} = 0.171$ (73)	0.0016	0.92
	H'_τ		$\mu_{\tau 0} = 1.09$ (74)	$\mu_{\tau 1} = -0.062$ (88)	$\mu_{\tau 2} = 0.0054$ (26)		$\mu_{\tau 3} = -0.37$ (41)	$\mu_{\tau 4} = 0.53$ (29)	0.025	0.93
	H_ρ		$\mu_{\rho 0} = 0.80$ (17)	$\mu_{\rho 1} = -0.039$ (21)	$\mu_{\rho 2} = 0.0012$ (6)		$\mu_{\rho 3} = 0.001$ (10)	$\mu_{\rho 4} = 0.239$ (68)	0.0014	0.95
	H_τ		$\mu_{\tau 0} = 0.37$ (57)	$\mu_{\tau 1} = 0.054$ (68)	$\mu_{\tau 2} = 0.0012$ (20)		$\mu_{\tau 3} = -0.21$ (32)	$\mu_{\tau 4} = 0.39$ (22)	0.015	0.93
regression	s_ρ	(3 cost.)	$\nu_{\rho 0} = 2.92$ (26)	$\nu_{\rho 1} = -0.028$ (13)			$\nu_{\rho 2} = -0.10$ (15)		0.049	0.40
	s_τ		$\nu_{\tau 0} = 3.63$ (37)	$\nu_{\tau 1} = -0.074$ (19)			$\nu_{\tau 2} = -0.36$ (21)		0.099	0.63
regression	H'_ρ	(3 cost.)	$\mu_{\rho 0} = 0.38$ (5)	$\mu_{\rho 1} = 0.001$ (27)			$\mu_{\rho 3} = 0.292$ (30)		0.0021	0.89
	H'_τ		$\mu_{\tau 0} = -0.48$ (21)	$\mu_{\tau 1} = 0.115$ (11)			$\mu_{\tau 3} = 0.36$ (12)		0.032	0.91
	H_ρ		$\mu_{\rho 0} = 0.42$ (6)	$\mu_{\rho 1} = -0.001$ (23)			$\mu_{\rho 3} = 0.330$ (32)		0.0022	0.91
	H_τ		$\mu_{\tau 0} = -0.05$ (15)	$\mu_{\tau 1} = 0.092$ (8)			$\mu_{\tau 3} = 0.327$ (87)		0.017	0.92

[a] Standard errors for μ and ν coefficients are given in parentheses.

guishable from one with say $m \approx 10$). The ls fit was then repeated fixing $m = 20$, either maintaining the condition $s_\rho = s_\tau = 2$ (Gauss profiles) or waiving the $s = 2$ conditions. In all cases the ls procedure was recycled until χ^2 = constant. The parameter shifts become always a very small fraction of their standard errors. The results of these calculations are summarized in Table I. As Figure 1 shows the agreement of calculated and observed profiles is quite satisfactory.

In the present case, as the number of analyzed reflections is fairly high, it is possible to inquire the dependence of the parameters of the empirical idf on the position on the film. It is indeed evident that the latter, and particularly the peak widths H_ρ and H_τ, are influenced by instrumental and morphological factors: crystal size and degree of orientation. This could be accomplished on the basis of theoretical relationships between peak widths and film coordinates, such as that given by Millane and Arnott[10] (this article came to author's attention after the completion of this work and gives only the formulas for the flat-camera technique). For the time being we have performed only an empirical analysis based on statistical methods with the purpose of verifying the feasibility of simple relationships practical for implementing the structure refinement program. We have referred to the polar coordinates of the reflection centers r_k,φ_k and evaluated (see Table II) the correlation coefficients and the coefficients of multiple regression[11] versus r_k and φ_k for $H_\rho^\bullet$, $H_\tau^\bullet$ (peak widths for $s = 2$), H_ρ, H_τ (peak widths for $s \neq 2$), s_ρ, and s_τ. H quantities (see Table II) exhibit strong correlation while s quantities are only weakly correlated. We decided therefore to perform a multiple regression versus r_k,φ_k of H and s values based on a polynomial of

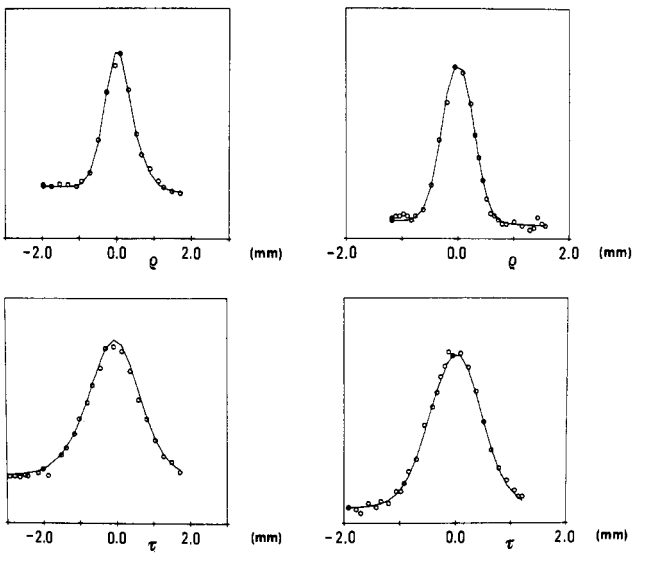

Figure 1. Fits of observed and calculated profiles are shown for reflections 113 + 023 (exactly overlapped, left) and 115 + 025 (exactly overlapped, right). In both cases sections along ρ-line (up) and along τ-lines (down) are considered. Intensities are in arbitrary units.

degree 2 for the H's and degree 1 for the s's.

$$H_\rho = \mu_{\rho 0} + \mu_{\rho 1} r_k + \mu_{\rho 2} r_k^2 + \mu_{\rho 3} \varphi_k + \mu_{\rho 4} \varphi_k^2 \quad (5a)$$

$$H_\tau = \mu_{\tau 0} + \mu_{\tau 1} r_k + \mu_{\tau 2} r_k^2 + \mu_{\tau 3} \varphi_k + \mu_{\tau 4} \varphi_k^2 \quad (5b)$$

$$s\rho = \nu_{\rho 0} + \nu_{\rho 1} r_k + \nu_{\rho 2} \varphi_k \quad (5c)$$

$$s_\tau = \nu_{\tau 0} + \nu_{\tau 1} r_k + \nu_{\tau 2} \varphi_k \quad (5d)$$

The regression for H parameters was performed twice by considering, alternatively, the values $H_\rho^\bullet$ and $H_\tau^\bullet$ obtained with the $s = 2$ condition imposed and the values H_ρ and H_τ obtained with the latter condition waived. The "best" μ and ν coefficients were determined by using again the least-square approach minimizing the sum $\sum(Y_{obsd} - Y_{calcd})^2$ ($Y = H$ or s) for the 28 observations listed in Table I (the last five regressions give two observations each). In each case it was considered the root-mean-square deviation S and the overall index of correlation R[11] (see Table II). From the results it is evident that the standard errors for μ and ν parameters based on the above regression formula are very high. So we have tried other regressions, also listed in Table II, with lesser parameters and found that H_ρ and H_τ can be expressed satisfactorily by $3 + 3$ μ values instead $5 + 5$ while $H_\rho^\bullet$ and $H_\tau^\bullet$ are not expressed as well (especially $H_\tau^\bullet$). The regression of s_ρ and s_τ (especially s_ρ) gives instead a weak dependence both on r_k and on φ_k suggesting the use of constant s values or, possibly, s_ρ constant and s_τ a linearly variable with r_k only. Furthermore only s_τ differs appreciably from 2, and also along τ the use of an $s \neq 2$ value gives only a modest improvement.

Conclusion

The present analysis has confirmed also for PIB diffraction spectra the feasibility of Gauss functions both for expressing the intensity distribution functions along constant-2ϑ lines and along variable-2ϑ lines. Statistical coefficients of regression have also shown that the dependence of peak widths on film position is close to a bilinear relationship against the polar coordinates of the peak.

In the following paper we shall report how—on the basis of this analysis—a structure refinement of PIB was performed by using the whole fiber diffraction pattern. We shall also discuss the importance of combining the whole-pattern approach with constrained refinement.

Acknowledgment. We are indebted to Prof. G. Zannotti, Università di Padova, for the use of Optronics photoscan instrument and for useful discussions. Financial support by Ministero della Pubblica Istruzione and Consiglio Nazionale delle Ricerche is also acknowledged.

Registry No. PIB, 9003-27-4.

References and Notes

(1) Immirzi, A.; Iannelli, P. *Gazz. Chim. Ital.* **1987**, *117*, 201.
(2) Immirzi, A.; Iannelli, P. *Macromolecules* **1988**, *21*, 768.
(3) Rietveld, H. M. *Acta Crystallogr.* **1967**, *22*, 151.
(4) Rietveld, H. M. *J. Appl. Crystallogr.* **1969**, *2*, 65.
(5) Tanaka, T.; Chatani, Y.; Tadokoro, H. *J. Polym. Sci., Polym. Phys. Ed.* **1974**, *12*, 515.
(6) Iannelli, P.; Immirzi, A. *Acta Crystallogr. Sect. A: Found Crystallogr.* **1987**, *A43*, C-199.
(7) Iannelli, P.; Immirzi, A. *Macromolecules*, following paper in this issue.
(8) Hall, M. M., Jr.; Veeraraghavan, V. G.; Rubin, H.; Winchell, P. G. *J. Appl. Crystallogr.* **1977**, *10*, 66.
(9) Ortega, J. M.; Reinholdt, W. C. *Iterative Solution of Nonlinear Equations in Several Variables*; Academic: New York, 1970.
(10) Millane, R. P.; Arnott, S. *J. Macromol. Sci., Phys.* **1985**, *B24*, 193.
(11) Wheaterburn, C. E. *A First Course in Mathematical Statistics*; Cambridge University: New York, 1977.

Structure Analysis of Polyisobutylene Based on the Whole-Pattern Fiber Diffraction Method. 2. Refinement of Structure Based on Several Constrained Models

Pio Iannelli and Attilio Immirzi*

Dipartimento di Fisica, Università di Salerno, I-84100 Salerno, Italy.
Received January 6, 1988; Revised Manuscript Received June 8, 1988

ABSTRACT: On the basis of the results of a spot-by-spot analysis of the X-ray fiber diffraction pattern of polyisobutylene the structure of this polymer has been refined according to the "whole-pattern" approach. The starting point was the structure by Tadokoro and the method used was that of "constrained refinement" considering fixed C–C bond lengths and free bond and torsion angles. It is shown that the whole-pattern approach is a practical tool for refining structures of fibrous materials also in cases of considerable structural complexity provided the number of unknowns is properly reduced. By assuming that all CMe_2–CH_2–CMe_2 chain bond angles are equal to each other as well as CH_2–CMe_2–CH_2 angles, one obtains the values 129° and 110° for the above bond angles with the eight chain torsional angles −48°, −168°, −60°, −157°, −54°, −167°, −54°, and −166°, in excellent agreement with previously obtained values.

Introduction

Structure refinement of crystalline fibrous materials can be undertaken, as discussed in the preceding paper,[1] by using the "whole-pattern" instead of "integrated" intensities. By using an empirical approach we have obtained for polyisobutylene (PIB) crystallized under stretching a number of peak parameters which allow for reproducing with sufficient accuracy the effective intensity distribution function (idf) for the X-ray diffraction pattern. On this basis the crystal structure can be refined by optimizing *both* structural parameters and peak parameters.

The whole-pattern approach, based on a least-square fitting procedure, has been outlined in previous papers.[2,3] The fit is performed by comparing the "observed" diffraction intensities $I_{obsd,i}$ with the ones calculated as $S\sum_k I_k \Omega_{ik}$ where S denotes a scale factor, i any measured

0024-9297/89/2222-0200$01.50/0